Supplementary material to
Crystalline microstructure of boehmites studied by multi-peak analysis of powder X-ray diffraction patterns

Pablo Pardo [1], Marek Andrzej Kojdecki [2], José Miguel Calatayud [1], José María Amigó [3] and Javier Alarcón [1]

[1] Department of Inorganic Chemistry, University of Valencia, Valencia, Spain
[2] Institute of Mathematics and Cryptology, Military University of Technology, Warsaw, Poland
[3] Department of Geology, University of Valencia, Valencia, Spain

A. XRD patterns

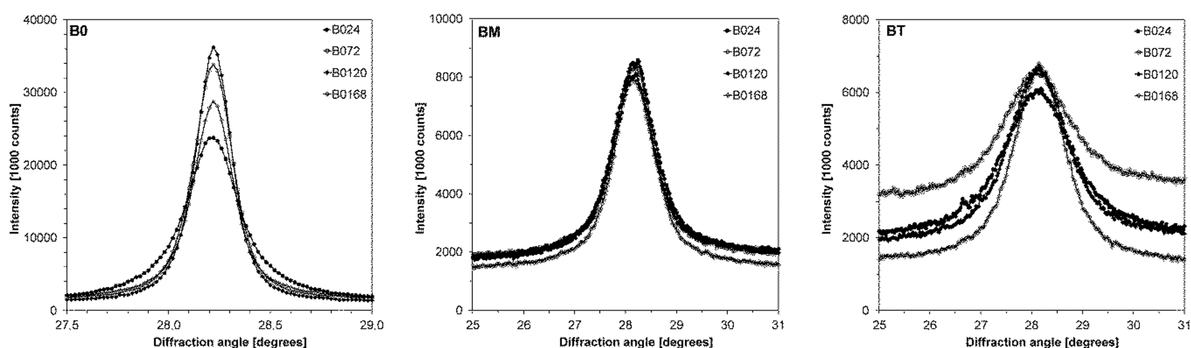

Figure S1 (a,b,c). XRD peaks for 120 reflection from all specimens as illustrating the influence of crystalline microstructure on XRD patterns.

B. Qualitative XRD analysis

A qualitative analysis of XRD patterns of the samples was performed by using Scherrer formula with the constant equal to 1 (the results are collected in Table SI and Table SII). In order to extract the line profile parameters of each sample (position, full-width-at-half-maximum, integral breadth and line shape) the Socabim fitting program PROFILE was used.

Table SI. XRD line profile parameters for the reflections considered in calculations with using Scherrer formula: 2θ – the peak position (in diffraction angle scale); β_f – the observed integral breadth.

Sample	020		120		031		200		002	
	2θ (°)	β_f (°)	2θ (°)	β_f (°)	2θ (°)	β_f (°)	2θ (°)	β_f (°)	2θ (°)	β_f (°)
B024	14.45	0.538	28.19	0.346	38.34	0.495	49.27	0.219	64.96	0.279
B072	14.47	0.175	28.19	0.185	38.34	0.274	49.28	0.139	64.97	0.216
B0120	14.48	0.140	28.20	0.157	38.34	0.246	49.28	0.120	64.97	0.189
B0168	14.48	0.174	28.19	0.196	38.34	0.255	49.28	0.163	64.97	0.204
BM24	14.31	2.099	28.15	1.346	38.32	1.186	49.17	0.596	64.91	0.666
BM72	14.37	2.074	28.12	1.353	38.30	1.182	49.16	0.592	64.90	0.667
BM120	14.30	1.865	28.14	1.339	38.31	1.152	49.19	0.487	64.91	0.712
BM168	14.38	1.869	28.15	1.228	38.32	1.172	49.19	0.578	64.91	0.646
BT24	14.25	2.129	28.10	2.125	38.30	1.596	49.16	1.458	64.85	1.206
BT72	14.26	2.129	28.12	2.125	38.30	1.242	49.16	1.249	64.87	1.160
BT120	14.28	2.129	28.11	1.837	38.29	1.389	49.19	1.018	64.89	0.871
BT168	14.37	1.970	28.12	1.642	38.31	1.411	49.19	0.969	64.88	0.882

Table SII. Results of the application of Scherrer equation: D_{hkl} – apparent crystallite sizes calculated in directions perpendicular to planes (020), (120), (031), (200), (002) from full-width-at-half-maximum of XRD line profiles for corresponding reflections; with – averaged value and crystallite shape coefficients.

Sample	D_{020} (nm)	D_{120} (nm)	D_{031} (nm)	D_{200} (nm)	D_{002} (nm)	(nm)	D_{020}/D_{200}	D_{002}/D_{200}
B024	16.5	26.3	18.9	44.3	37.4	28.7	0.37	0.84
B072	50.7	49.1	34.1	70.0	48.4	50.5	0.72	0.69
B0120	63.5	57.9	38.0	81.0	55.3	59.1	0.78	0.68
B0168	51.2	46.4	36.6	59.7	51.3	49.0	0.86	0.86
BM24	4.2	6.8	7.9	16.3	15.7	10.2	0.26	0.96
BM72	4.3	6.7	7.9	16.4	15.7	10.2	0.26	0.96
BM120	4.8	6.8	8.1	19.9	14.7	10.9	0.24	0.74
BM168	4.8	7.4	8.0	16.8	16.2	10.6	0.29	0.96
BT24	4.2	4.3	5.9	6.7	8.7	6.0	0.63	1.30
BT72	4.2	4.3	7.5	7.8	9.0	6.6	0.54	1.15
BT120	4.2	5.0	6.7	9.5	12.0	7.5	0.44	1.26
BT168	4.5	5.5	6.6	10.0	11.9	7.7	0.45	1.19

High resolution transmission electron microscopy (HRTEM) images and electron diffraction diagrams were collected using a Tecnai G2 F20 field emission electron microscope equipped with a Gatan CCD camera. Data treatment was performed with Digital Micrograph software.

C. Dependence of XRD pattern on crystalline microstructure characteristics of model polycrystal and inverse problem

The XRD pattern depends implicitly on the microstructure of investigated specimen. Therefore the model parameters, characterising a real polycrystalline material, may be recovered from XRD data through describing this dependence and solving the corresponding inverse problem. The pure line profiles, f_{hkl}, containing all accessible information on specimen microstructure, must be extracted from non-overlapping experimental line profiles, h_{hkl}, by using standard line profiles, g_{hkl}, (both after background subtraction), as solutions of a convolution integral equation of the first kind:

$$\int_{-\sigma}^{+\sigma} g_{hkl}(s-t)\, f_{hkl}(t)\, dt = h_{hkl}(s) \qquad \text{(S1)}$$

for each *hkl* reflection, corresponding to a Bragg angle $\vartheta_{0,hkl}$; where s is the reciprocal lattice vector length, $s \approx 4\pi\lambda^{-1}(\vartheta - \vartheta_{0,hkl})\cos\vartheta_{0,hkl}$, λ is the X-ray wavelength and σ is the sufficiently large number (Wilson, *The Mathematical Theory of X-Ray Powder Diffractometry*, 1963). In turn, in the frame of this model each pure line profile in the vicinity of a Bragg angle may be treated as the convolution of two hypothetic functions – one, k_{hkl}, originating only from the shape and size distribution of crystallites, and the other, r_{hkl}, originating only from the strain distribution:

$$\int_{-\sigma}^{+\sigma} k_{hkl}(s-t)\, r_{hkl}(t)\, dt = f_{hkl}(s), \quad k_{hkl}(s) = \int_0^N \Psi_{hkl}(n,s)\, v(n)\, dn \text{, or}$$

$$\int_{-\sigma}^{+\sigma} \left[\int_0^N \Psi_{hkl}(n, s-t)\, v(n)\, dn \right] r_{hkl}(t)\, dt = f_{hkl}(s) \qquad \text{(S2)}$$

with a volume-weighted crystallite size distribution v and a second-order crystalline lattice strain distribution r (for example: Kojdecki *et al.*, 2007, Kojdecki *et* al., 2009), under the assumption that the structure factor is constant for all crystallites. For assumed crystallite shape and fixed n, function $\Psi_{hkl}(n,s) = n^{-3}\Phi_{hkl}(n,s)$ describes the pure diffraction line (*hkl* reflection) from an individual crystallite (scattering X-rays coherently) with a perfect lattice and with the size

characterised by a number n (taken with weight n^{-3}); N must be sufficiently large (so that $v(n)=0$ for $n>N$).

The function r_{hkl} for each hkl reflection may be represented as being equal to the second-order crystalline lattice strain distribution r with changed argument: $r_{hkl}(\vartheta-\vartheta_{0,hkl})=r(-[\vartheta-\vartheta_{0,hkl}]\cot\vartheta_{0,hkl})$ which relates to a position shift $\vartheta_0\rightarrow\vartheta$ of a peak from a single crystallite. This shift corresponds to a relative change $\delta d/d_0=(d-d_0)/d_0$ of lattice parameters and interplanar spacings d (inside each crystallite): $\delta d/d\approx-(\vartheta-\vartheta_0)\cot\vartheta_0$, in accordance with the model assumption about the second-order strain form. In formulae (S1) and (S2) as well as in the others, both the reflection and diffraction angles are considered in radians.

Each investigated material is characterised by a prevalent crystallite shape, a volume-weighted crystallite size distribution and a second-order crystalline lattice strain distribution, computed from experimental data by simultaneous analysis of several line profiles extracted from XRD patterns. As a criterion of similarity of XRD profiles simulated (with using computed microstructure characteristics) to experimental ones (measured, after subtracting background), the weighted Euclidean norms are applied:

$$R_m(h_{hkl}^{meas},h_{hkl}^{calc})\equiv m^{-1}\sum_{hkl}\left\|h_{hkl}^{calc}-h_{hkl}^{meas}\right\|_2\left\|h_{hkl}^{meas}\right\|_2^{-1},\ \left\|h_{hkl}^{meas}\right\|_2\equiv\left[\sum(h_i)^2\right]^{1/2}\text{ or}$$

$$R_{wp}(h_{hkl}^{meas},h_{hkl}^{calc})\equiv\left[m^{-1}\sum_{hkl}\left\|h_{hkl}^{calc}-h_{hkl}^{meas}\right\|_2^2\left\|h_{hkl}^{meas}\right\|_2^{-2}\right]^{1/2},\ \left\|h_{hkl}^{meas}\right\|_2\equiv\left[\sum(h_i)^2\right]^{1/2}\qquad\text{(S3)}$$

where m is the number of simultaneously analysed peaks (included in summation with corresponding indices); peak maximums are treated as free variables. Microstructure characteristics of a sample under study are computed by solving system of equations (S1) and (S2) with using regularisation method to minimise approximately second functional (S3).

Each size distribution determined from experimental data is tested whether can it be well approximated to a bimodal logarithmic-normal (LN) distribution, $p=c_1p_1+c_2p_2$, of components being densities of LN probability distributions with parameters γ_i, ω_i:

$$p_i(x)=(x\omega_i\sqrt{2\pi})^{-1}\exp\left[-(\ln x-\gamma_i)^2(2\omega_i^2)^{-1}\right],\qquad\text{(S4)}$$

with the mean $\mu_i=\exp(\gamma_i+0.5\omega_i^2)$ and the standard deviation $\sigma_i=\mu_i\left[\exp(\omega_i^2)-1\right]^{1/2}$ ($i=1$ or $i=2$). Attributing these components (S4) to two different crystallite fractions, one can determine the volume content of each fraction in the specimen total volume, c_i (while $\int_0^{+\infty}p(x)\,dx=c_1+c_2=1$). An unimodal LN distribution is included into this model by admitting $c_1=1,\ c_2=0$.

Each strain distribution determined from experimental data is tested whether it can be well approximated by an even function (with the mean value equal to zero) with positive parameters y (a multiplier scaling the function integral to unity), z and w: Pearson's curve of type II (S5) or Pearson's curve of type VII (S6)

$$\Omega:\quad p(t)=y\left[\max\left\{0,(1-t^2z^{-2})\right\}\right]^w,\qquad\text{(S5)}$$

$$\Delta:\quad p(t)=y\left[(1+t^2z^{-2})^w\right]^{-1}.\qquad\text{(S6)}$$

In computations the crystallites were modelled as spheres, cylinders (of rotation axis in the [001] direction), or orthorhombic prisms (with edges parallel to axes [100], [010] and [001] and different aspect ratios). The pure line profile from an individual crystallite, $\Phi_{hkl}(n,s)$, is the Fourier transform of its scattering efficiency $\Xi_{hkl}(n,m)$ (Wilson, 1963). If the number of pairs of unit cells spaced by $|m|$ interplanar distances, $|m|d_{hkl}$, in the direction perpendicular to the diffracting planes (hkl) in a crystallite is equal to $\Xi_{hkl}(n,m)$, then

$$\Phi_{hkl}(n,s)=\int_{-\infty}^{+\infty}\Xi_{hkl}(n,m)\exp(isd_{hkl}m)\,dm\ . \qquad \text{(S7)}$$

For a parallelepiped-crystallite with edges parallel to the principal crystal axes and with a perfect crystalline lattice,

$$\Xi_{hkl}(n,m)=\begin{cases}E\,(n-|m|HG^{-1})(n-|m|KG^{-1})(n-|m|LG^{-1}) & \text{for } |m|<M\\ 0 & \text{for } |m|\ge M\end{cases}; \qquad \text{(S8)}$$

$$\begin{aligned}\Phi_{hkl}(n,s)=E\,(sd)^{-4}\Big\{&\big[2(nsd)^3\,(1-(H+K+L)F^{-1}+(HK+HL+KL)F^{-2}-HKLF^{-3})\\ &+4nsd\,(3HKLF^{-1}-(HK+HL+KL))G^{-2}\big]\sin(GF^{-1}nsd)\\ +&\big[2(nsd)^2(-(H+K+L)+2(HK+HL+KL)F^{-1}-3HKLF^{-2})\,G^{-1}+12HKLG^{-2}\big]\cos(GF^{-1}nsd) \qquad \text{(S9)}\\ +&\big[2(nsd)^2(H+K+L)G^{-1}-12HKLG^{-2}\big]\Big\} \qquad \text{for } s\neq 0,\end{aligned}$$

$$\Phi_{hkl}.(n,0)=E\cdot 2n^4G(1-2^{-1}(H+K+L)F^{-1}+3^{-1}(HK+HL+KL)F^{-2}-4^{-1}HKLF^{-3}).$$

For the orthorhombic lattice (when a parallelepiped becomes a prism), if the prism edge lengths along [100], [010] and [001] axes are equal to na , κnb and ηnc (where *a*, *b*, *c* are the unit cell parameters, κ and η are the shape coefficients), then symbols *F*, *G*, *H*, *K*, *L* have the following meaning for Miller indices h,k,l: $E=a\kappa b\eta c$, $F=\max(H,K,L)$, $M=GF^{-1}n$, $d=d_{hkl}=aG^{-1/2}$ is the interplanar distance for (hkl) planes and:

$$G=h^2+a^2b^{-2}k^2+a^2c^{-2}l^2\ ,\ H=h\ ,\ K=\kappa^{-1}a^2b^{-2}k\ ,\ L=\eta^{-1}a^2c^{-2}l\ . \qquad \text{(S10)}$$

The full-width-at-half-maximum (FWHM) in reflection angle scale of a profile from a parallelepiped-crystallite is approximately equal to

$$\left[\frac{1-\frac{1}{2}\frac{H+K+L}{F}+\frac{1}{3}\frac{HK+HL+KL}{F^2}-\frac{1}{4}\frac{HKL}{F^3}}{\frac{1}{3}-\frac{1}{4}\frac{H+K+L}{F}+\frac{1}{5}\frac{HK+HL+KL}{F^2}-\frac{1}{6}\frac{HKL}{F^3}}\right]^{\frac{1}{2}}\frac{F}{\sqrt{G}}\,\frac{0.584\lambda}{\pi a\cos\vartheta_{0,hkl}}\,\frac{1}{n} \qquad \text{(S11)}$$

with the relative accuracy within 0.028 (M.A. Kojdecki, *Materials Science Forum*. **443-444** (2004), 107-110). To compare, for a spherical crystallite with diameter na the FWHM is equal to $0.554\lambda/(na\cos\vartheta_{0,hkl})$ (within 0.001). Formulae similar to (S10) were elaborated also for parallelepiped-crystallites of other crystallographic systems. Formulae similar to (S8) – (S11) were elaborated also for cylindrical, spherical and hexagonal-prismatic crystallites.

D. Characteristics of crystalline microstructure of studied boehmite specimens

In this chapter the averaged characteristics of crystalline microstructure of all boehmite specimens are presented in diagrams.

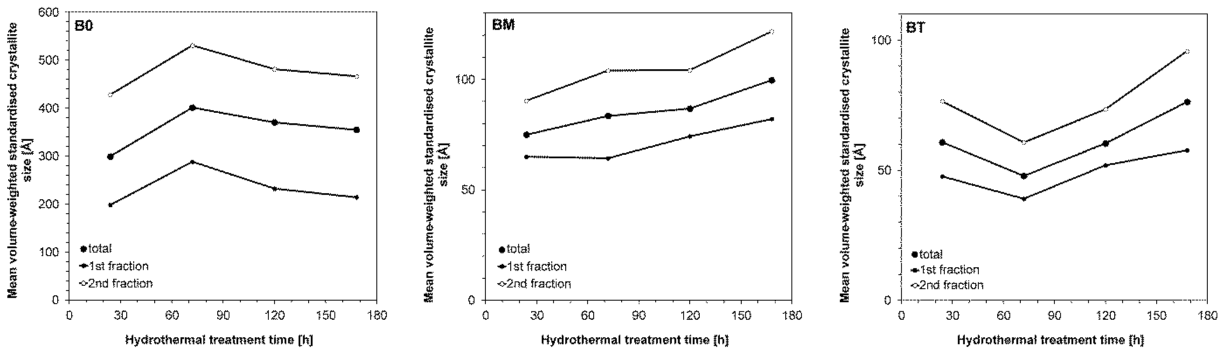

Figure S2. Mean standardised crystallite size as a function of hydrothermal treatment time for B0 (a), BM (b) and BT (c) samples.

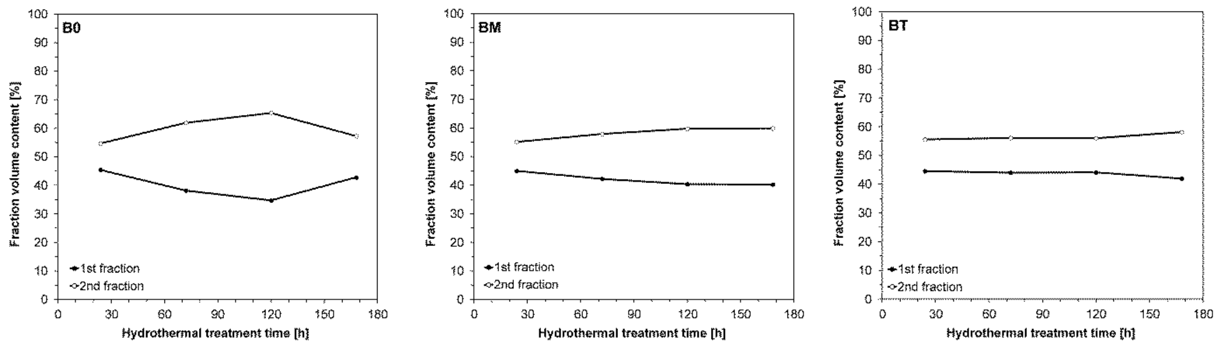

Figure S3. Fraction volume as a function of hydrothermal treatment time for B0 (a), BM (b) and BT (c) samples.

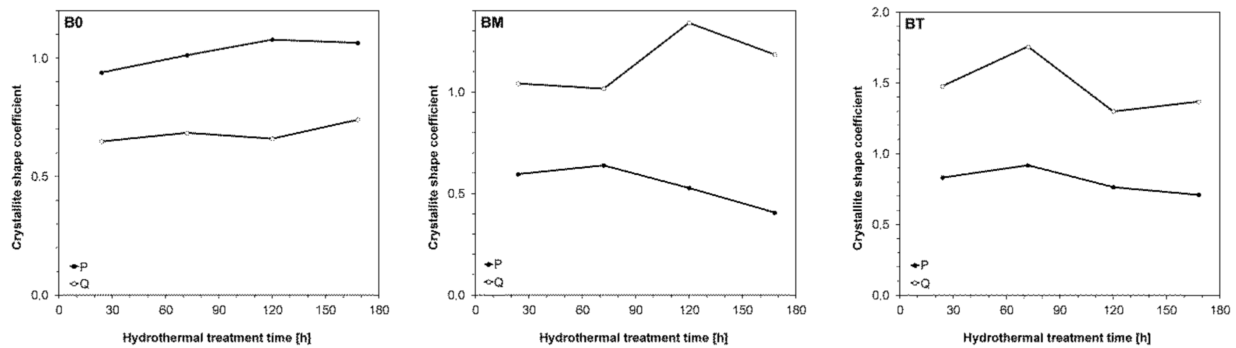

Figure S4. Crystallite shape coefficients as functions of hydrothermal treatment time for B0 (a), BM (b) and BT (c) samples.

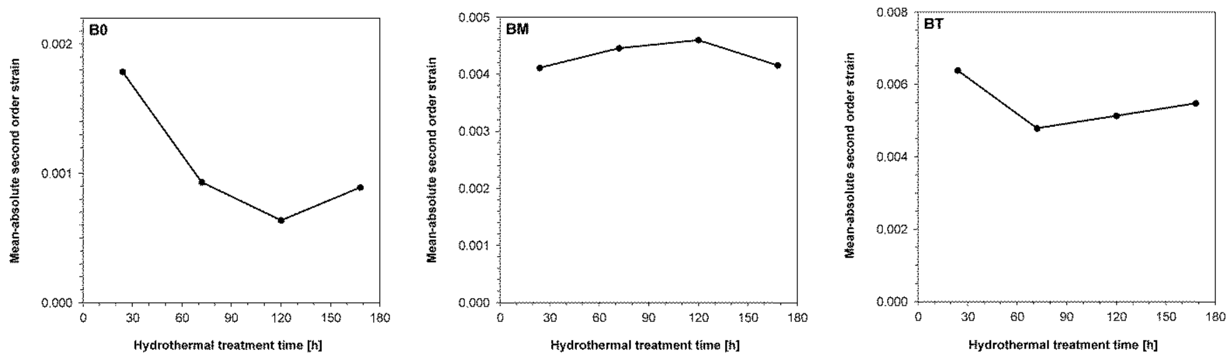

Figure S5. Mean-absolute second-order crystalline lattice strain as a function of hydrothermal treatment time for B0 (a), BM (b) and BT (c) samples.

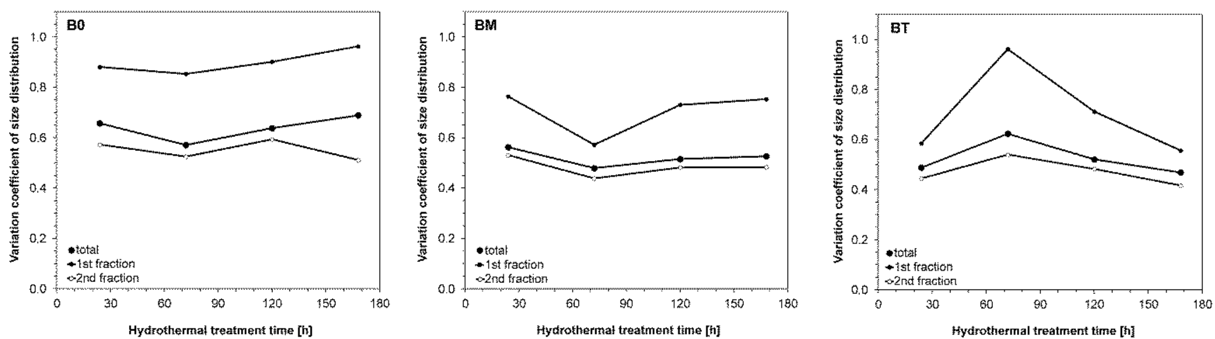

Figure S6. Variation coefficient of crystallite size distribution as a function of hydrothermal treatment time for B0 (a), BM (b) and BT (c) samples.

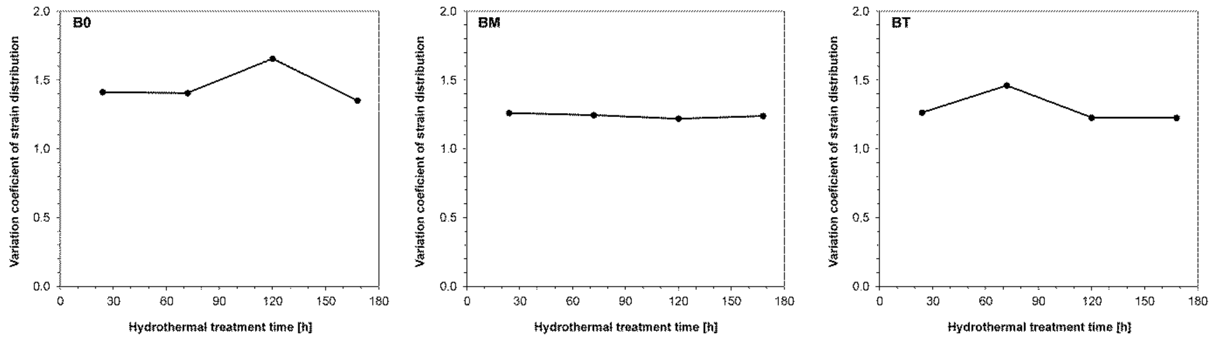

Figure S7. Variation coefficient of second-order strain distribution as a function of hydrothermal treatment time for B0 (a), BM (b) and BT (c) samples.

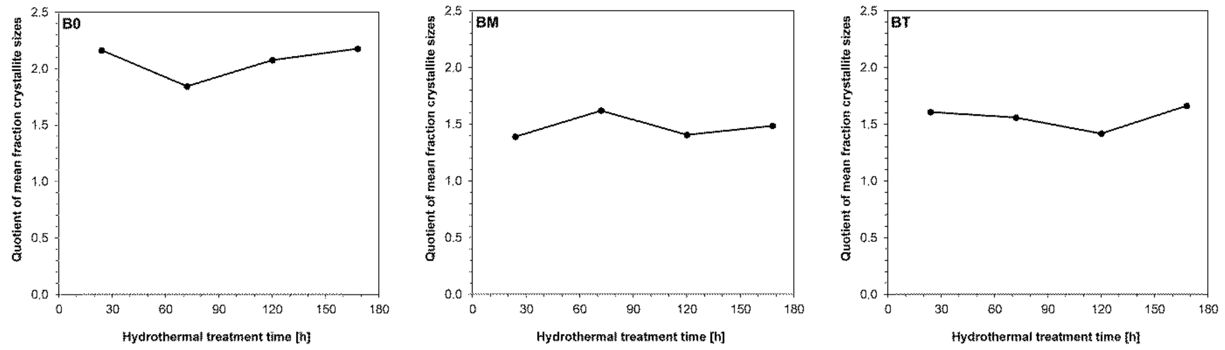

Figure S8. Quotient of mean fraction crystallite sizes as a function of hydrothermal treatment time for B0 (a), BM (b) and BT (c) samples.